Available online at www.sciencedirect.com

ScienceDirect

journal homepage: www.elsevier.com/locate/issn/15375110

Research Paper

Prototype semi-transparent photovoltaic modules for greenhouse roof applications

Akira Yano [a,*], Mahiro Onoe [b], Josuke Nakata [c]

[a] Faculty of Life and Environmental Science, Shimane University, 1060 Nishikawatsu, Matsue, Shimane 690-8504, Japan

[b] Graduate School of Life and Environmental Science, Shimane University, 1060 Nishikawatsu, Matsue, Shimane 690-8504, Japan

[c] Kyosemi Corporation, Fushimi, Kyoto 612-8201, Japan

ARTICLE INFO

Article history:
Received 20 September 2013
Received in revised form
19 March 2014
Accepted 1 April 2014
Published online 22 April 2014

Keywords:
Solar cell
Renewable energy
Spherical
Shading
Cover material
Plant

Improved energy efficiency and the increased use of renewable energy are important objectives for sustainable greenhouse crop production. Two prototypes of semi-transparent-bifacial photovoltaic modules intended for greenhouse roof applications were developed. A module (PV_1) using 1500 spherical solar microcells (1.8 mm diameter, crystalline silicon) with 15.4 cells cm^{-2} density in 108 mm × 90 mm area was produced. Thirty-nine percent of the area was covered with the cells. The remaining 61% was transparent to allow the most sunlight to enter the greenhouse for promising plant photosynthesis. Similarly, a module (PV_2) was made using 500 cells with 5.1 cells cm^{-2} density. Thirteen percent of the area of this module was covered with the cells. The peak power output was 540 mW when the PV_1 module was irradiated with 1213 W m^{-2} sunlight coming directly from the sky and via ground reflection. The peak power output was 202 mW when the PV_2 module was irradiated with 1223 W m^{-2} sunlight. The conversion efficiencies from sunlight energy irradiated on the 108 mm × 90 mm area into electrical energy were 4.5% for the PV_1 module and 1.6% for the PV_2 module. Calculations of the annual electrical energy production per unit greenhouse land area indicated that these modules are potentially suitable for greenhouses in high-irradiation regions where electricity production could be high and winter demand low.

1. Introduction

Greenhouse plant production improves the yield and quality of crops through control of the growth environment in terms of light, water, temperature, relative humidity, CO_2 concentration, and ventilation. Greenhouse environment control often entails the consumption of fuel and electricity. Consequently, important aims for sustainable greenhouse crop production are to minimise energy consumption and to compensate, or partly compensate, the consumed energy with renewable energy (Bot et al., 2005; Yano et al., 2009, 2010).

* *Corresponding author*. Tel./fax: +81 852 32 6543.
E-mail address: yano@life.shimane-u.ac.jp (A. Yano).

http://dx.doi.org/10.1016/j.biosystemseng.2014.04.003

Nomenclature

d	distance between the PV module and an observation point in the PV cell shadow, m
e_1	solar eclipsing percentage by PV_1 cells, %
e_2	solar eclipsing percentage by PV_2 cells, %
I	electric current, A
I_{HT}	global irradiance on a horizontal plane, W m^{-2}
I_{HS1}	horizontal global irradiance in the PV_1 cell shadow, W m^{-2}
I_{HS2}	horizontal global irradiance in the PV_2 cell shadow, W m^{-2}
I_T	global irradiance on the inclined PV top surface, W m^{-2}
$I_{T\rho}$	ground-reflected irradiance on the inclined PV bottom surface, W m^{-2}
p	atmospheric transmissivity, %
P_{max}	peak power value of a P_{pv}–V characteristic curve of the PV modules, W
P_{pv}	power output of the PV modules, W
s_0	shading percentage of the PV-module's transparent cover materials, %
V	voltage, V
β	tilt angle of the PV modules, °
γ	angle between direct sunlight incidence and the sky-directing PV-module's normal, °
η	module efficiency, %
ψ_p	azimuth of the PV module's normal from the south, °

Crop yields depend strongly on the availability of light. Nearly 1% yield loss is expected to occur with a 1% reduction in light (Kläring & Krumbein, 2013; Marcelis, Broekhuijsen, Meinen, Nijs, & Raaphorst, 2006). Nevertheless, in some high-irradiation regions or during summer for some crop species, solar radiation is often too intense. Accordingly, screens and coating applications are used to moderate the intensity of radiation in greenhouses (López-Marín, Gálvez, González, Egea-Gilabert, & Fernández, 2012). This fact implies that the excessive sunlight irradiating greenhouses could be useful to provide an electrical energy source for the operation of environment-control equipment after conversion into electricity using photovoltaic (PV) modules.

Yano et al. (2005b) and Yano, Tsuchiya, Nishi, Mariyama, and Ide (2007) developed a ventilation window controller driven solely by electrical energy supplied from a greenhouse-roof-mounted 0.078 m^2 PV-module with a conventional 28 Ah car battery used for PV energy storage. The stand-alone ventilation-window controller was operated successfully and greenhouse temperature was regulated appropriately. This implies that a PV module size could be extended to cover more of the greenhouse roof and that heavier electrical loads than the ventilation window controller could be driven using PV generated electricity. If the electrical energy consumed by some heavy loads, such as heating and cooling, could be replaced, or partially replaced, by PV generated energy, then the consumption of grid-supplied electricity in greenhouses could be reduced. Yano et al. (2010) studied electricity gain and shading in an east–west oriented greenhouse on which a 720 W maximum-rated-power PV array covering 12.9% of the roof area was mounted. Two PV array configurations were tested: a straight-line and checkerboard arrangements. The two arrangements created quite different sunlight distributions in the greenhouse, although the electrical energy generated by these two arrangement PV arrays was comparable. The annual solar-irradiation distribution in the checkerboard PV greenhouse was more uniform than that of the straight-line PV greenhouse because the checkerboard PV array intermittently cast shadows in the greenhouse. Kadowaki, Yano, Ishizu, Tanaka, and Noda (2012) studied how plants grew in the greenhouse equipped with the PV arrays. The growth of welsh onions under the straight-line arranged PV array shadows was inhibited significantly because the PV array cast shadows on the plants continuously during cultivation. However, the inhibitory growth effects of the shading were diminished with the checkerboard array. The PV results were not generalised because the balance between the amount of electricity produced and the allowable shading rate varies according to plant species, geography, meteorology, season, and greenhouse characteristics. Ureña-Sánchez, Callejón-Ferre, Pérez-Alonso, and Carreño-Ortega (2012) tested PV modules with a checkerboard arrangement for greenhouse tomato production with nearly 10% coverage. The results showed that PV shading did not affect the yield or the price of tomatoes despite some negative effects on fruit size and colour.

The use of sunlight can be shared by plants and PVs by separating the sunlight spectrum with respect to plant photosynthesis and PV electricity production. The sunlight spectrum in the 400–700 nm wavelength range is designated as the photosynthetically active radiation (PAR) because it is particularly important for crop cultivation. Radiation with wavelengths longer than 700 nm could be useful for purposes other than plant cultivation. Consequently, Sonneveld, Swinkels, Bot, and Flamand (2010) and Sonneveld, Swinkels, Campen, et al. (2010) developed a greenhouse roof PV system that allowed the penetration of PAR for plant growth but captured near-infrared radiation for electricity production and heat storage. Another aspect of solar radiation is beam density: i.e. direct and diffused irradiance. Fresnel-lens greenhouse roofs have been developed to concentrate the direct radiation onto a photovoltaic and thermal collection module, while diffused radiation remains unchanged and reaches the plants (Sonneveld et al., 2011; Souliotis, Tripanagnostopoulos, & Kavga, 2006).

These studies showed that although conscientious design is necessary, it is possible to generate enough electricity for the control of greenhouse environment appliances using PV systems that are compatible with plant cultivation (Kadowaki et al., 2012; Sonneveld et al., 2011; Ureña-Sánchez et al., 2012; Wenger & Teitel, 2012).

Past PV greenhouse studies commonly used conventional flat hard or planar flexible PV modules (Al-Ibrahim, Al-Abbadi, & Al-Helal, 2006; Kadowaki et al., 2012; Pérez-Alonso, Pérez-García, Pasamontes-Romera, & Callejón-Ferre, 2012; Sonneveld, Holterman, Swinkels, van Tuijl, & Bot, 2008; Sonneveld, Swinkels, Bot, et al., 2010; Sonneveld, Swinkels, Campen,

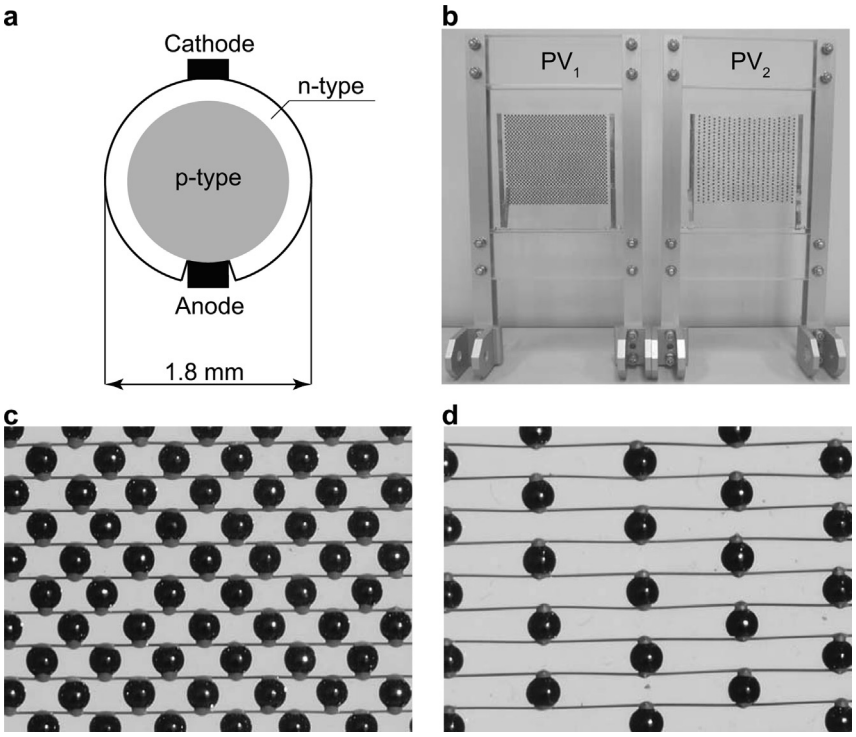

Fig. 1 – Cross-sectional structure of the spherical solar microcell (Sphelar®, a) and the prototype PV modules (b) with 15.4 cells cm^{-2} (PV_1, c) or 5.1 cells cm^{-2} (PV_2, d) cell density.

et al., 2010; Sonneveld et al., 2011; Sugiura, Yano, Tsuchiya, Iimoto, & Tagawa, 2002; Ureña-Sánchez et al., 2012; Yano, Furue, et al., 2007; Yano et al., 2005a, 2009, 2010). However, recent progress in PV cell technologies has provided additional possibilities for solar cell applications in greenhouses. A spherical solar microcell is one such candidate that is notable for its small size and its isotropic ability for photoreception (Biancardo et al., 2007). Although roof and wall orientations differ among greenhouses, spherical cells have no directional preference. For this reason, the cell is expected to produce

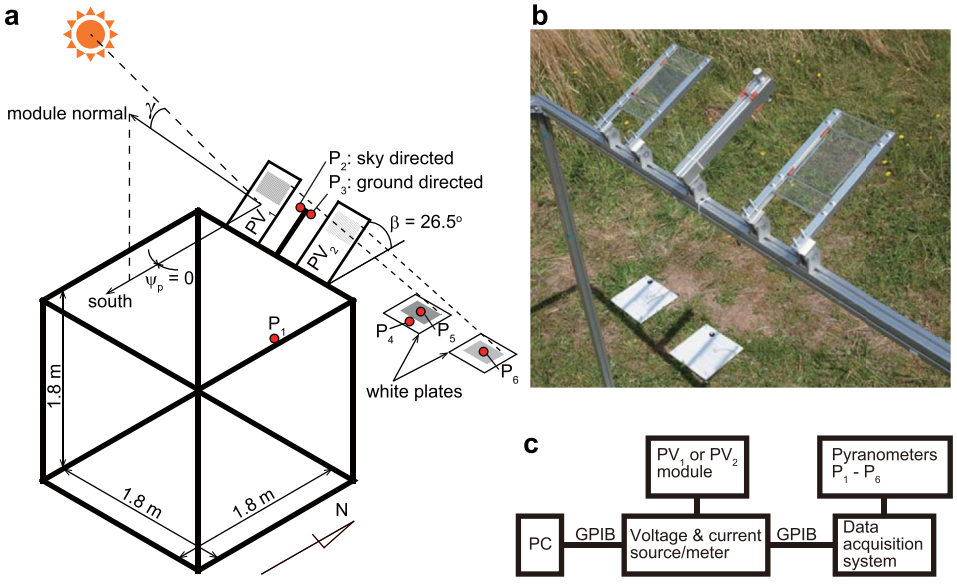

Fig. 2 – Configuration of sunlight, shading, and PV module output measurements. PV_1 and PV_2 modules and pyranometers P_1, P_2, and P_3 (a) were mounted 2 m above the wild-plant covered ground (b), on which two horizontal white plates had been positioned for tracking the PV cell shadows. P_5 and P_6 respectively measured I_{HS1} and I_{HS2}. P_4 was positioned at the margin of the PV_1 cell shadow. All pyranometer and PV module output data were stored synchronously in the PC through the GPIB interface (c).

constant quantities of electricity over widely differing sunlight incident angles. Consequently, they are suitable for greenhouse-roof and greenhouse-wall embedded appli cations.

This study developed two types of prototype PV modules, in which spherical solar microcells of 1.8-mm diameter (Taira & Nakata, 2010) were embedded with different levels of cell densities to produce electrical energy without severe shading of greenhouse crops. The small size of the spherical cell is an advantage since a single cell does not completely eclipse the sun when observed from below thus avoiding the direct shading sunlight on the plants.

2. Materials and methods

2.1. *Spherical solar microcells and the semi-transparent PV modules*

Crystalline silicon spherical solar microcells of 1.8 mm diameter (Sphelar®; Kyosemi Corp., Kyoto, Japan) were used (Fig. 1a). The PV cells were composed of a p-type semiconductor as the inner core and an n-type semiconductor as the outer shell. The power output is drawn through the electrodes. The maximum power output of the single cell is 0.48 mW. The optimum operating voltage is 0.48 V. The optimum operating current is 1.01 mA. The light–electricity conversion efficiency is 18.9% (Nakata, 2003) for standard evaluation conditions (1 kW m^{-2} single side irradiation; 25 °C) with air mass 1.5, a typical solar spectrum on the earth's surface on a clear day (Markvart, 2000, chap. 2).

A module (PV_1) was made using 1500 cells with 15.4 cells cm^{-2} density (Fig. 1b and c). In the PV_1 module, 30 cells with 1.8 mm mutual separation were aligned in straight lines so that every anode of the 30 cells was soldered directly to a straight wire of 0.1-mm diameter and every cathode was soldered to another straight wire (see Fig. 1c). As a result, the 30 cells were connected electrically in parallel. Repeating this process, 10 pairs of the 30 parallel cells were connected electrically in series. Finally, five pairs of the 10 series connections were connected in parallel. The 1500 cells were sandwiched between 4-mm-thick glass plates after they

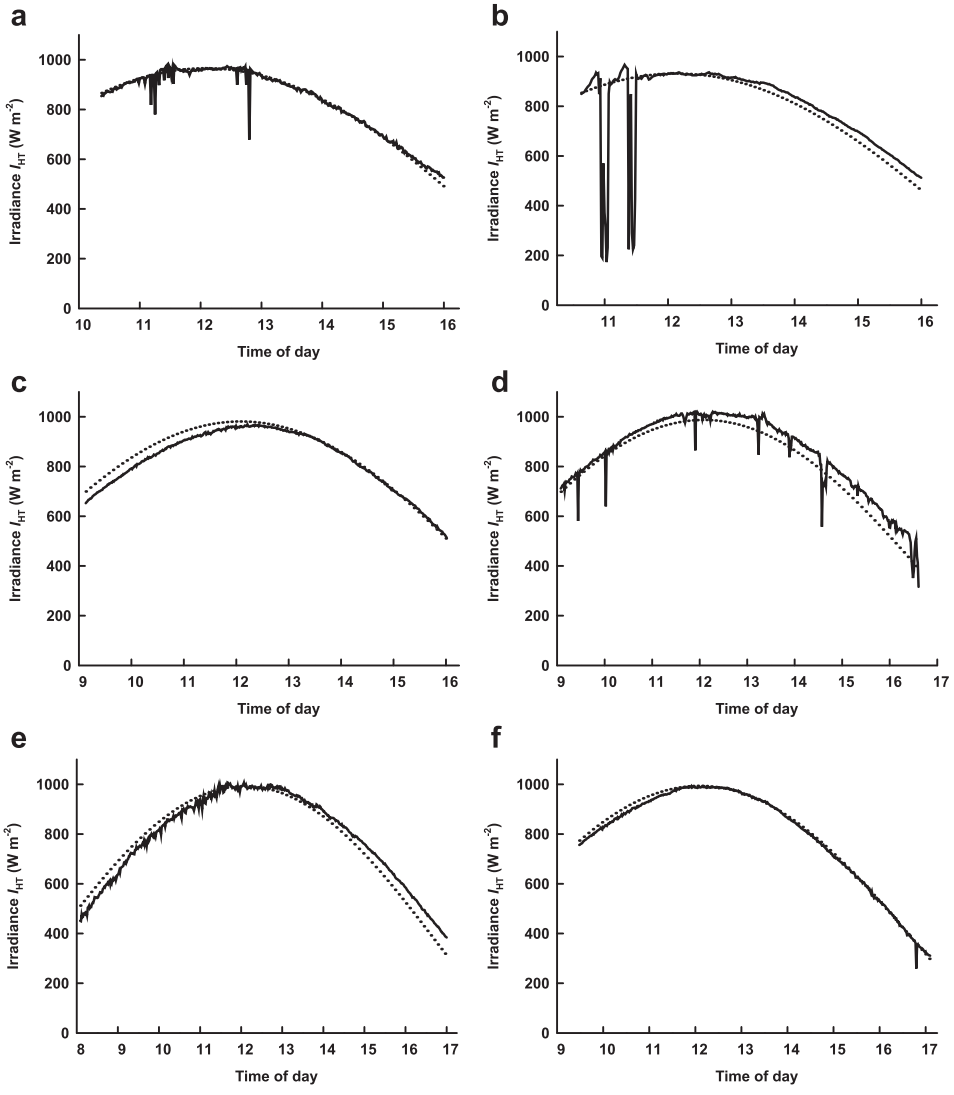

Fig. 3 – Measured (solid lines) and calculated (dotted lines) global irradiance on the horizontal plane I_{HT} on 5 May (a), 22 April (b), 13 May (c), 17 May (d), 21 May (e), and 22 May (f). Atmospheric transmissivity $p = 0.65$ was used for calculations.

were embedded in 3-mm-thick transparent resin. The 1500 cells were distributed across a 108 mm × 90 mm area. Thirty-nine percent of the area was covered with the cross-sectional area of the 1500 cells. Similarly, a module (PV_2) was made using 500 cells with 5.1 cells cm^{-2} density (Fig. 1b and d). The 500 cells were distributed in a 108 mm × 90 mm area, 13% of which was covered with the cross-sectional area of the 500 cells. In the PV_2 module, 10 cells with 9.0 mm mutual separation were connected in parallel using the 0.1-mm-diameter wire. Then 10 pairs of the 10 parallel connected cells were connected in series. Finally, five pairs of the 10 parallel × 10 series cell array were connected in parallel.

2.2. Electrical and shading characteristics of the semi-transparent PV modules

The electrical and shading characteristics of the PV_1 and PV_2 modules were measured at a grass plot on the Shimane University campus (35°29′N, 133°04′E) during several sunny days in 2013 (Fig. 2). The current I–voltage V characteristics of the PV_1 module were measured at 1 min intervals from 10:22 through 16:00 on 5 May using a voltage and current source/meter (6241A; ADC Corp., Tokyo, Japan; Fig. 2c). The PV_1 and PV_2 modules were supported 2 m above the ground by aluminium frames. Both PV modules were inclined 26.5° (β), which is a common tilt angle of glass greenhouses in the Shimane area. The azimuth of the PV-module's sky-directing normal coincided with the upper culmination direction ($\psi_p = 0°$; Fig. 2a). The PV_2 module was positioned next to the PV_1 module to measure the shading percentage only. Similarly, the I–V characteristics of the PV_2 module were measured during 10:37–15:59 on 22 April. The global irradiance on the inclined PV-module's top surface I_T and the ground-reflected irradiance on the inclined PV-module's bottom surface $I_{T\rho}$ were measured at 1 min intervals using pyranometers P_2 and P_3 (ML-020VM; Eko Instruments Co. Ltd., Tokyo, Japan), which were positioned on the top and bottom of a 26.5° inclined bar (Fig. 2a and b). The shadows of the 108 mm × 90 mm semi-transparent cell areas of the PV_1 and PV_2 modules were detected using two 300 mm × 300 mm white plates placed horizontally on the ground (Fig. 2a and b). As the shadows moved, the white plates were moved by

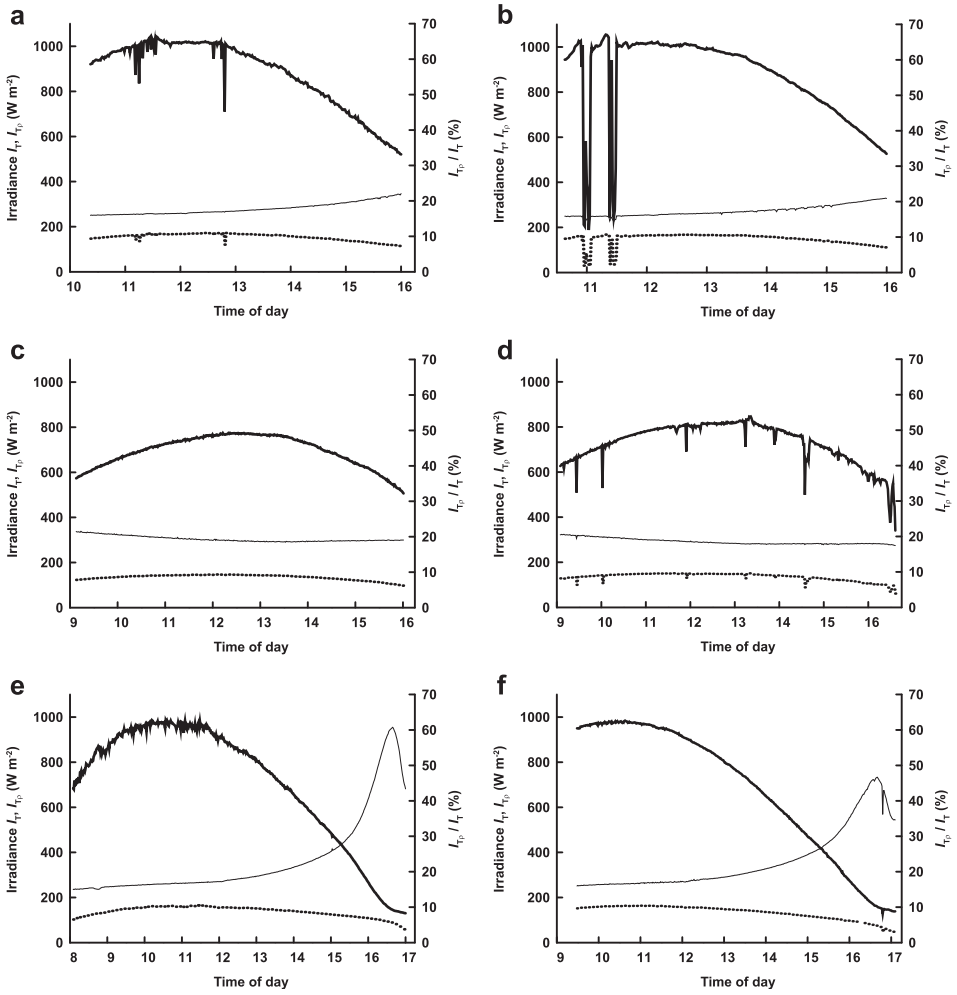

Fig. 4 – Global sky irradiances I_T on the 26.5° inclined PV-modules' top-surfaces (bold solid lines), ground-reflected irradiances $I_{T\rho}$ on the PV-modules' bottom surfaces (dotted lines), and the $I_{T\rho}/I_T$ percentage (fine solid lines) on 5 May (a), 22 April (b), 13 May (c), 17 May (d), 21 May (e), and 22 May (f). The PV modules' top surfaces were directed to the south sky on 5 May and 22 April, to the north sky on 13 and 17 May, and to the east sky on 21 and 22 May.

hand to shade the pyranometers on the white plates. This tracking procedure was conducted during a pause during data logging to avoid the pyranometers being shaded by human intervention. The global irradiances I_{HS1} and I_{HS2} refer to the respective shadows of the semi-transparent PV_1 and PV_2 cell areas on the horizontal plates and were measured at 1 min intervals using pyranometers P_5 and P_6 (ML-020VM). Pyranometer P_4 was positioned at the margin of the PV_1 cell shadow to measure the shading percentage of the PV module's transparent cover materials (layers of glass and resin outside the cell area). Pyranometer P_1 (ML-020VM) was positioned horizontally 2 m above the ground to measure the horizontal global irradiance I_{HT} at 1 min intervals. The electrical characteristics and the irradiance data were transmitted through a GPIB interface and stored synchronously in a computer.

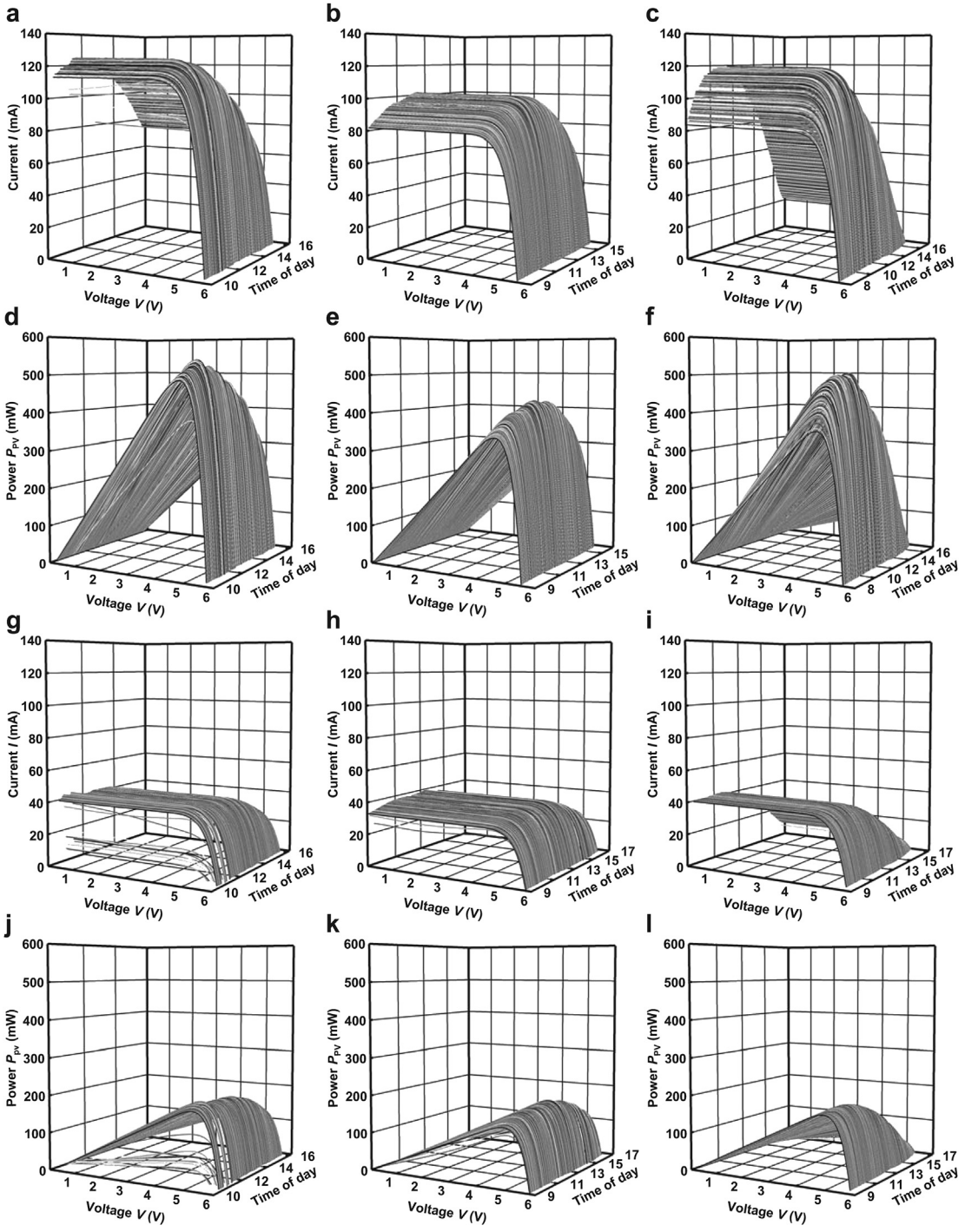

Fig. 5 – I–V (a, b, c, g, h, and i) and P_{PV}–V (d, e, f, j, k, and l) characteristics of the PV_1 (a–f) and PV_2 (g–l) modules. The PV modules' top surfaces were directed southward to the sky (a, d, g, and j), to the north sky (b, e, h, and k), or to the east sky (c, f, i, and l).

The PV_1 module was directed northerly towards the sky ($\psi_p = 180°$) at the inclination (β) of 26.5° between 9:07 and 16:00 on 13 May to measure the I–V characteristics. Pyranometers P_2 and P_3 were also directed respectively to the northern sky and the southern ground at $\beta = 26.5°$. Similarly, the I–V characteristics of the PV_2 module facing to the northern sky were measured during 9:04–16:36 on 17 May. The I–V characteristics of the eastern sky facing ($\psi_p = -90°$) PV_1 and PV_2 modules inclined 26.5° were measured respectively during 8:05–17:00 on 21 May and during 9:28–17:05 on 22 May.

The module efficiency η was defined as the percentage of the PV module's power output P_{pv} to the impinging irradiance $I_T + I_{T\rho}$ on the 108 mm × 90 mm semi-transparent cell area. The spectral irradiances from the top and bottom surfaces of the PV modules were measured using a spectroradiometer (MS-720; Eko Instruments Co. Ltd., Tokyo, Japan). The theoretical values of γ, defined as the angle between the direct beam sunlight irradiating on the PV module and the PV-module's upper normal, was calculated at 1 min intervals for the experimental date and site. I_{HT}, I_T, and $I_{T\rho}$ were also calculated theoretically (Yano et al., 2009).

3. Results and discussion

During the experiment sky conditions were fair with occasional clouds. However, the atmospheric transparency was not good. This condition is typical in this area during this season. The measured global irradiance on the horizontal plane I_{HT} is shown in Fig. 3 for each date. The peak I_{HT} values were around 1000 W m^{-2} at culmination. Calculation approximated the measured I_{HT} curves when the atmospheric transmissivity p was assumed as 0.65 (dotted lines in Fig. 3).

Figure 4 shows the global irradiance on the inclined PV-module's top surface I_T, the ground-reflected irradiance on the inclined PV-module's bottom surface $I_{T\rho}$, and the percentage of $I_{T\rho}$ to I_T. The I_T value of the southern facing PV modules exceeded 1000 W m^{-2} around culmination (Fig. 4a and b). The ratio $I_{T\rho}/I_T$ was 14–22%. Although I_{HT} reached 1 kW m^{-2} at culmination (Fig. 3c and d), the I_T values at culmination were only 800 W m^{-2} for the north-facing PV modules (Fig. 4c and d) because direct sunlight impinged on the PV module surface with greater γ than those of the south-facing modules. The ratio $I_{T\rho}/I_T$ remained 17–22%. The I_T values of the east-facing PV modules reached 1000 W m^{-2} around 10–11 h. The percentage of $I_{T\rho}/I_T$ exceeded 50% at dusk. Direct sunlight did not irradiate the PV module surfaces when the $I_{T\rho}/I_T$ percentage peaked at dusk because the direct beam was perpendicular to the PV module normal. Although $I_{T\rho}$ is not useful at all for conventional single-side flat PV modules, $I_{T\rho}$ contributes effectively to the electricity production of the present bifacial PV modules.

Figure 5 depicts the I–V and the power output P_{PV}–V characteristics of the PV_1 and PV_2 modules measured at 1 min intervals. The peak currents of the PV_1 module (Fig. 5a–c) were threefold greater than those of the PV_2 module (Fig. 5g–i) for respective PV module orientations. Correspondingly, the peak powers of the PV_1 module (Fig. 5d–f) were threefold greater than those of the PV_2 module (Fig. 5j–l) for respective PV module orientations. The north-facing PV modules (Fig. 5b, e, h, and k) generated about 80% of the electricity generated by the south-facing PV modules (Fig. 5a, d, g, and j), indicating the merit of using the isotropic solar microcells in greenhouse north roofs. I_T peaked in 10–11 h for the east-facing PV modules, causing I and P_{PV} peaks at that time period (Fig. 5c, f, i, and l). The maximum peak value P_{max} of the PV_1 module's P_{PV}–V curve was 540 mW at 11:34 on 5 May when the PV_1 module faced south. At that moment, $I_T + I_{T\rho}$ was 1213 W m^{-2}, the open circuit voltage was 5.59 V, the short circuit current was 125 mA, the optimum operating voltage was 4.62 V, the optimum operating current was 117 mA, and the fill factor was 0.77, where the product of the optimum operating voltage and current provides the maximum power output of the PV module. The fill factor is defined as the ratio of the product of the optimum operating voltage and current to the product of the open circuit voltage and the short circuit current (Markvart, 2000, chap. 2). A higher fill factor corresponds to a higher efficiency. The maximum P_{max} value of the PV_2 module was 202 mW at 11:18 on 22 April when the PV_2 module faced the sky southwards. At that moment, $I_T + I_{T\rho}$ was 1223 W m^{-2}, the open circuit voltage was 5.87 V, the short circuit current was 43 mA, the optimum operating voltage was 4.93 V, the optimum operating current was 41 mA, and the fill factor was 0.80. Figure 6a shows the relationship between P_{max} and

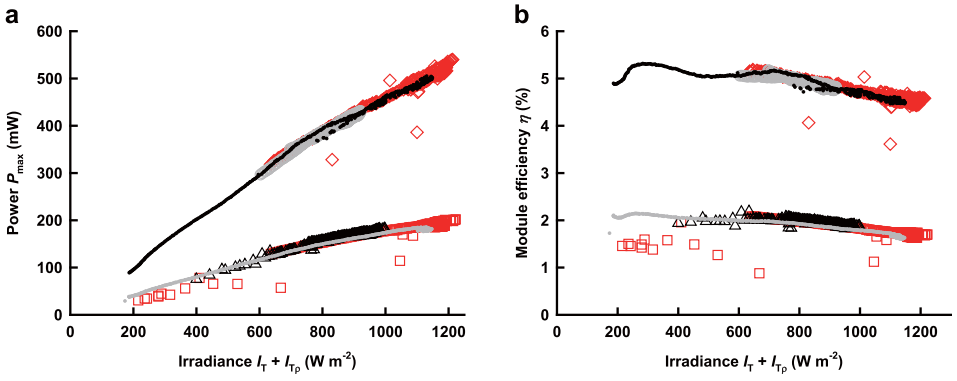

Fig. 6 – Relation between peak PV power output P_{max} and $I_T + I_{T\rho}$ (a) of the south-sky facing PV_1 (open red diamonds) and PV_2 (open red squares), the north-sky facing PV_1 (open grey circles) and PV_2 (open black triangles), and the east-sky facing PV_1 (black dots) and PV_2 (grey dots), and the relation between module efficiency η and $I_T + I_{T\rho}$ (b).

$I_T + I_{T\rho}$. Irrespective of the PV module orientation, P_{max} increased with the increase of $I_T + I_{T\rho}$ on a single curve. The P_{max} values of the PV_1 module were about three times greater than those of the PV_2 module through the whole $I_T + I_{T\rho}$ range. The efficiency values η of the PV_1 and PV_2 modules were, respectively, 5% and 2%, but these values decreased slightly with increased $I_T + I_{T\rho}$ (Fig. 6b). This reason is discussed in the next paragraph in relation to the sunlight incident angle, although an increase in the module temperature might be another cause of the decrease in η.

Figure 7a depicts the calculated angle γ between the direct sunlight incidence and the sky-directing PV-module's normal during each experiment. The γ values were 3–58° for the south-facing modules, 43–63° for the north-facing modules, and 11–93° for the east-facing modules. η increased slightly with increased γ (Fig. 7b). This phenomenon corresponds to the increase in η with decreased $I_T + I_{T\rho}$ (Fig. 6b). The instability of η can be explained by the directionality of the accuracy of the pyranometer: the incident solar irradiance can be underestimated at large γ (up to 17% error at $\gamma > 60°$ according to the pyranometer manual). When γ values are large, the pyranometer underestimates I_T. That underestimation of I_T results in an overestimation of η because η is proportional to the inverse of $I_T + I_{T\rho}$. The power output P_{pv} of the isotropic PV cells can be maintained at a high value at a large γ, resulting in a high η at a large γ. For the best accuracy, $\eta = 4.5\%$ at $\gamma = 7.4°$, which was the minimum incident angle of direct solar irradiance, was determined as the efficiency of the PV_1 module. Similarly, $\eta = 1.6\%$ at $\gamma = 3.1°$ was determined as the efficiency of the PV_2 module. Figure 7c presents the relationship between P_{max} and γ. When γ was 7.4°, P_{max} of the PV_1 module was 519 mW. When γ was 3.1°, P_{max} of the PV_2 module was 188 mW. P_{max} for the east-facing PV_1 module took dual values around $\gamma = 20°$ (the black dots in Fig. 7c) because the module received direct sunlight from the equivalent γ angles twice before and after 10:00, but solar irradiance increases as the solar elevation angle increases toward its culmination. Thus, P_{max} values after 10:00 were greater than those before 10:00. In contrast, the P_{max} values overlapped on the single curve for the south-facing and north-facing PV modules because both the $I_T + I_{T\rho}$ and γ values are symmetrical with respect to the culmination.

Annual electrical energy production per unit land area of a symmetrical shape greenhouse mounted the PV cells on its entire or half side roof with PV_1 ($\eta = 4.5\%$) or PV_2 ($\eta = 1.6$) module density was calculated assuming the present location (35°29′N, 133°04′E), cloudless sky, 0.20 of albedo, $p = 0.65$, $\beta = 26.5°$ (Table 1). If the PV_1 modules cover the entire roof of an east–west oriented greenhouse, then system will produce 102 kWh m^{-2} yr^{-1}. If only the north roof is covered with the PV_1 modules, then the system will produce 39 kWh m^{-2} yr^{-1}. This value is slightly greater than that from PV_2 modules covering the entire roof. When the PV_1 modules cover the entire roof of a north–south oriented greenhouse, the system would produce 110 kWh m^{-2} yr^{-1}. This value is greater than that of the PV_1 modules covering the entire roof of the east–west oriented greenhouse. If the entire roof of a north–south oriented greenhouse was covered with PV_2 modules, then similar electrical energy to that of PV_1 modules covering the north roof of the east–west oriented greenhouse would be produced. Table 2 presents calculations of the annual electrical energy consumption per unit greenhouse land area of various greenhouse locations and electrical loads from several reports in the literature. Data deviated from 2 to 20 kW m^{-2} yr^{-1} among greenhouses of the Mediterranean

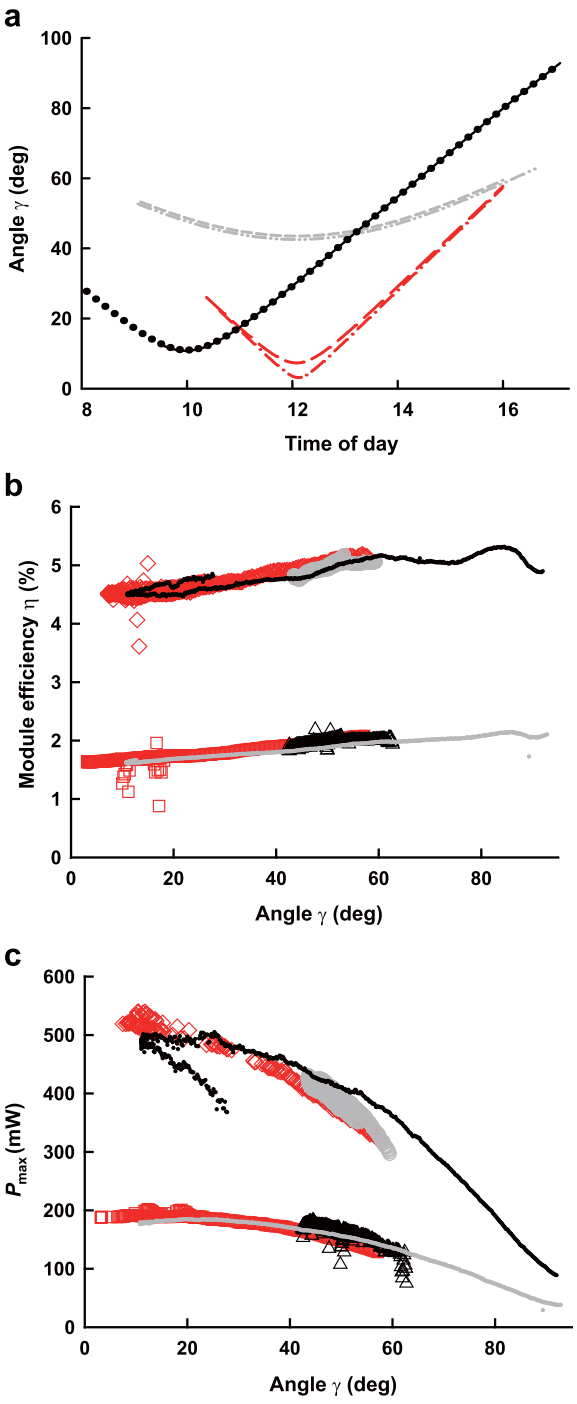

Fig. 7 – (a) Calculated angle γ of the south-sky facing PV_1 (red long-dashed line) and PV_2 (red dotted-dashed line), the north-sky facing PV_1 (grey dashed line) and PV_2 (grey double-dotted dashed line), and the east-sky facing PV_1 (black dotted line) and PV_2 (black solid line) modules; (b) relation between η and γ; (c) the relation between P_{max} and γ (symbols are as depicted in Fig. 6).

Table 1 – Estimation of annual electrical energy production by PV_1 and PV_2 modules mounted on greenhouse roofs.

Greenhouse orientation	PV module	PV roof coverage	Annual electrical energy production per unit greenhouse area[a] (kWh m^{-2} yr^{-1})
East–west	PV_1	South roof only	64
		North roof only	39
		South and north roofs	102
	PV_2	South roof only	23
		North roof only	14
		South and north roofs	36
North–south	PV_1	East or west roof only	55
		East and west roofs	110
	PV_2	East or west roof only	20
		East and west roofs	39

[a] $p = 0.65$; albedo = 0.20; cloudless sky; $\beta = 26.5°$; present study location (35°29′N, 133°04′E).

region, mainly because of differences in types of appliances with different power consumption and operating durations. The PV_1 and PV_2 modules are therefore considered suitable for greenhouses located in highly-irradiated regions where greater electricity production and less winter electricity demand are expected. Although the data in Table 1 were calculated with an assumption of cloudless skies, the PV_2 modules mounted on the north roof of an east–west oriented greenhouse can produce twice the electrical energy that would be consumed in a high irradiation greenhouse having necessary loads (Rocamora & Tripanagnostopoulos, 2006), suggesting that an adequate amount of electrical energy would be produced even under actual sky conditions where, to a certain degree, clouds obscure the sun.

When the sun was near culmination on 5 May, shadows of the semi-transparent PV cell area and the transparent PV module cover materials were tracked manually by pyranometers P_4, P_5, and P_6, which were positioned horizontally on white square plates (Fig. 2a and b). Figure 8 shows the measured shading percentages of the transparent PV module structure and the semi-transparent PV cell area. For $\gamma < 10°$, the mean shading percentage (s_0) of the transparent PV module structure was 9%. The mean shading percentages of the PV_1 and PV_2 cell area were, respectively, 43% and 23%. The shading percentage remained a constant value in $\gamma < 20°$ because of the low reflection of sunlight on the glass surface and the lack of overlapping of solar microcells.

Figure 9 shows the calculated relation between the sun eclipsing percentage by the PV_1 cells (e_1) and the PV_2 cells (e_2) and distance d between the PV module and observation points in the PV cell shadow. The inset photographs were taken at $d = 1.4$ m through an eclipsing observation filter mounted on a digital camera lens. Some examples of eclipsing patterns are also presented. At $d = 0.19$ m, the cross-sectional area of the sun projected on the PV modules coincides with the cross-sectional area of a single PV cell, resulting in perfect shading of direct beam sunlight at the observation point. As d increases, the eclipsing percentages converge to $e_1 = 39\%$ and $e_2 = 13\%$. Considering $s_0 = 9\%$ (Fig. 8), the direct-irradiance shading percentages of the PV_1 and the PV_2 modules converge respectively to 45% and 21%. This estimation well explains the measured shading percentages (Fig. 8). Assuming the application of the PV modules to greenhouse roofs, plants can be isolated more than 1 m distant from the roofs. For this reason, practically speaking, the percentage of eclipsed direct irradiance can be estimated as the percentage of the cross-sectional area of all cells to the PV module area. This assured semi-transparency of the direct solar irradiance onto plants is a particular merit of this type of micro solar cell. Earlier PV greenhouse studies (Kadowaki et al., 2012; Yano

Table 2 – Literature survey of annual electrical energy consumption per unit greenhouse area at different locations with electrical loads.

Location	Electrical load	Annual electrical energy consumption per unit greenhouse area (kWh m^{-2} yr^{-1})	Reference
Mediterranean	heating, cooling, ventilation	2–9	Campiotti et al. (2008)
Spain	window operation, pumps	3[a]	Ureña-Sánchez et al. (2012)
Spain	fans, irrigation and fertilisation equipment, fuel burner, window-opening and screen motors, automatism for climate control, compressor, electric resistance of the fuel reservoir	7	Rocamora and Tripanagnostopoulos (2006)
Greece	ventilation, cooling, lighting	20	Souliotis et al. (2006)
Saudi Arabia	fans, cooling pump, PC	56	Al-Ibrahim et al. (2006)
Sweden	ventilation, pumps, lighting and other devices	140	Vadiee and Martin (2013)

[a] Eight month data.

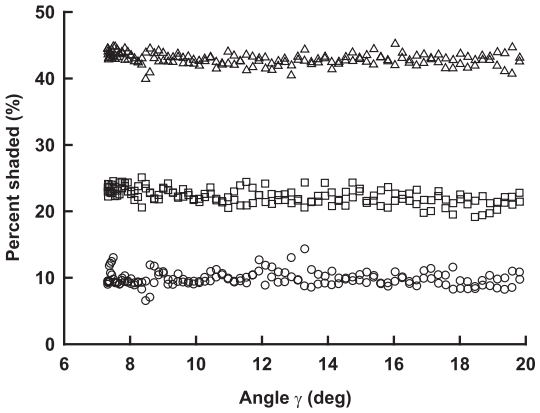

Fig. 8 – Measured shading percentages of global irradiation on the horizontal plane by the PV_1 cells (open triangles), PV_2 cells (open squares), and the transparent module materials (open circles).

et al., 2010) used a conventional planar PV modules, which were sufficiently large to completely shade direct irradiation, causing rapid changes of solar irradiation in the greenhouse. This can be avoided using micro-solar cells but solar scattered irradiance in a greenhouse covered with micro-solar cells depends on the rate of the cross-sectional areas of all cells to the entire greenhouse cover area. Accordingly, assuming that a greenhouse roof and walls are made entirely of the PV_1 or PV_2 modules, 45% or 21% of scattered irradiance can be shaded. If only a part of a greenhouse is covered by the PV modules, then the shading rate is decreased.

Figure 10a depicts spectral irradiance of the sunlight irradiated from the south sky and the north ground at 11:41 on 5 May, 2013. The ground-reflected irradiance is particularly low in PAR wavelength because ground-covering wild plants (Fig. 2b) absorbed PAR. A similar situation would occur when the PV modules are applied to greenhouse roofs, although this inference should be confirmed in future studies. The albedo was high at near-infrared wavelengths. Fortunately, the efficiency of the solar microcell peaks at 900 nm wavelength (Inagawa, 2005). This wavelength characteristic is suitable for use in greenhouse covers. The near-infrared albedo increased in the combination of the north sky and the south ground (Fig. 10b) measured at 12:01 on 13 May. Consequently, using ground-reflected solar irradiance for electricity production is efficient for the north roof application of bifacial PV modules.

Experiments should be conducted with greenhouses to evaluate the modification of light intensity and spectrum caused by greenhouse structures and crops as well as possible contamination of module surfaces by dust and agrochemicals. Reduction of the module thickness and enlargement of the module area that can be compatible with conventional greenhouse glass are necessary to set the PV modules for greenhouses. To reduce the thickness, downsizing of the spherical cells is also necessary. The cost of these prototype PV modules is extremely high because complex manufacturing processes that depend on manual work. The cost of production could be reduced considerably by automation.

4. Conclusions

This study examined electrical and shading characteristics of the prototype semi-transparent PV modules, which are intended to provide electrical energy consumed in greenhouses for plant environment control. PV modules of two types have been developed using different patterns of 1.8 mm spherical solar microcells. Single cells are so small that they do not entirely eclipse the sun when observed more than 0.19 m away from the module. For this reason, if the PV modules are applied to a greenhouse roof, then plants in the greenhouse being further away would not be shaded completely by the PV cells. Because of the isotropic

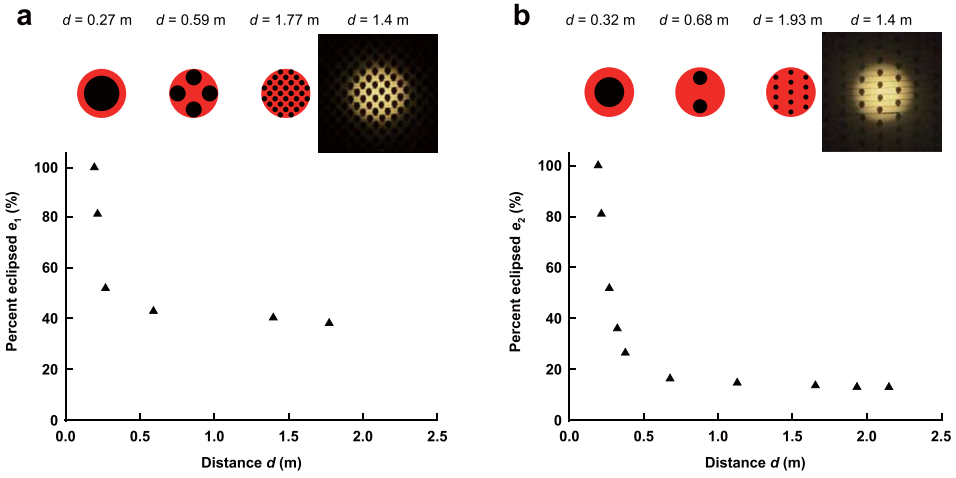

Fig. 9 – Calculated relation between the sun eclipsing percentage by spherical solar microcells and distance *d* between the PV_1 module and observation points that are positioned in the cell shadows (a) and between the PV_2 module and observation points (b). Some examples of eclipsing patterns are presented along with the photographs. The cross-sectional areas of the sun projected on the PV module and the solar microcells are depicted respectively as red and black circles. (For interpretation of the references to colour in this figure legend, the reader is referred to the web version of this article.)

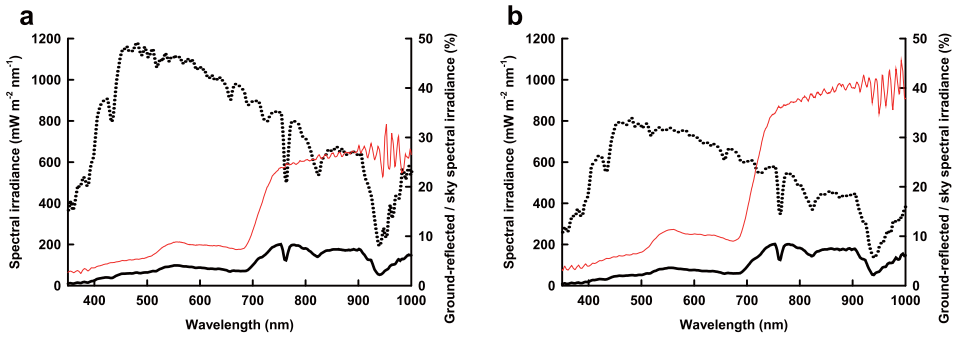

Fig. 10 – (a) Spectral irradiances impinged on the 26.5° inclined south-sky-facing PV module's top surface (dotted line) and bottom surface (black-bold solid line), and percentage of bottom surface/top surface spectral irradiance (red solid line); (b) spectral irradiances impinged on the 26.5° inclined north-sky-facing PV module's top and bottom surfaces, and their percentage (symbols are the same as (a)).

photoreception of the PV spherical cells, the modules are suitable for application in greenhouse as cover materials. Conventional single-side planar PV modules do not have this advantage. The PV_1 module design has threefold higher cell density than that of the PV_2 module, which gives it three times the electricity production and also shading. Comparing the module outputs with the electrical energy demands of several greenhouses quoted in the literature, the PV_1 and PV_2 modules are suitable for greenhouses in high-irradiation regions fitted with basic electrical environment control systems.

Acknowledgements

We thank Mr. Yasunori Katsumata and Mr. Yukinari Doi of Shimane University for their help in conducting the experiments. This study was supported by JSPS KAKENHI Grant Number 24580370.

REFERENCES

Al-Ibrahim, A., Al-Abbadi, N., & Al-Helal, I. (2006). PV greenhouse system – system description, performance and lesson learned. *Acta Horticulturae, 710*, 251–264.

Biancardo, M., Taira, K., Kogo, N., Kikuchi, H., Kumagai, N., Kuratani, N., et al. (2007). Characterization of microspherical semi-transparent solar cells and modules. *Solar Energy, 81*, 711–716.

Bot, G., van de Braak, N., Challa, H., Hemming, S., Rieswijk, Th, Straten, G. v., et al. (2005). The solar greenhouse: state of the art in energy saving and sustainable energy supply. *Acta Horticulturae, 691*, 501–508.

Campiotti, C., Dondi, F., Genovese, A., Alonzo, G., Catanese, V., Incrocci, L., et al. (2008). Photovoltaic as sustainable energy for greenhouse and closed plant production system. *Acta Horticulturae, 797*, 373–378.

Inagawa, I. (2005). Development and practical application of spherical micro silicon solar cell. *Journal of the Surface Finishing Society of Japan, 56*(1), 18–21 (in Japanese).

Kadowaki, M., Yano, A., Ishizu, F., Tanaka, T., & Noda, S. (2012). Effects of greenhouse photovoltaic array shading on Welsh onion growth. *Biosystems Engineering, 111*(3), 290–297.

Kläring, H.-P., & Krumbein, A. (2013). The effect of constraining the intensity of solar radiation on the photosynthesis, growth, yield and product quality of tomato. *Journal of Agronomy and Crop Science, 199*, 351–359.

López-Marín, J., Gálvez, A., González, A., Egea-Gilabert, C., & Fernández, J. A. (2012). Effect of shade on yield, quality and photosynthesis-related parameters of sweet pepper plants. *Acta Horticulturae, 956*, 545–552.

Marcelis, L. F. M., Broekhuijsen, A. G. M., Meinen, E., Nijs, E. M. F. M., & Raaphorst, M. G. M. (2006). Quantification of the growth response to light quantity of greenhouse grown crops. *Acta Horticulturae, 711*, 97–104.

Markvart, T. (Ed.). (2000). *Solar electricity* (2nd ed.). Chichester: John Wiley & Sons.

Nakata, J. (2003). Spherical solar cells solve issue of 3-D sunlight reception. *Asia Electronics Industry*, 45–48. February.

Pérez-Alonso, J., Pérez-García, M., Pasamontes-Romera, M., & Callejón-Ferre, A. J. (2012). Performance analysis and neural modelling of a greenhouse integrated photovoltaic system. *Renewable and Sustainable Energy Reviews, 16*, 4675–4685.

Rocamora, M. C., & Tripanagnostopoulos, Y. (2006). Aspects of PV/T solar system application for ventilation needs in greenhouses. *Acta Horticulturae, 719*, 239–246.

Sonneveld, P. J., Holterman, H. J., Swinkels, G. L. A. M., van Tuijl, B. A. J., & Bot, G. P. A. (2008). Solar energy delivering greenhouse with an integrated NIR filter. *Acta Horticulturae, 801*, 703–710.

Sonneveld, P. J., Swinkels, G. L. A. M., Bot, G. P. A., & Flamand, G. (2010). Feasibility study for combining cooling and high grade energy production in a solar greenhouse. *Biosystems Engineering, 105*(1), 51–58.

Sonneveld, P. J., Swinkels, G. L. A. M., Campen, J., van Tuijl, B. A. J., Janssen, H. J. J., & Bot, G. P. A. (2010). Performance results of a solar greenhouse combining electrical and thermal energy production. *Biosystems Engineering, 106*(1), 48–57.

Sonneveld, P. J., Swinkels, G. L. A. M., van Tuijl, B. A. J., Janssen, H. J. J., Campen, J., & Bot, G. P. A. (2011). Performance of a concentrated photovoltaic energy system with static linear Fresnel lenses. *Solar Energy, 85*(3), 432–442.

Souliotis, M., Tripanagnostopoulos, Y., & Kavga, A. (2006). The use of Fresnel lenses to reduce the ventilation needs of greenhouses. *Acta Horticulturae, 719*, 107–114.

Sugiura, H., Yano, A., Tsuchiya, K., Iimoto, M., & Tagawa, A. (2002). A model experiment for a plastic house ventilator driven by electricity from photovoltaic generators. *Journal of the Japanese Society of Agricultural Machinery, 64*(6), 128–136 (in Japanese with English abstract).

Taira, K., & Nakata, J. (2010). Silicon cells: catching rays. *Nature Photonics Technology Focus, 4*, 602–603.
Ureña-Sánchez, R., Callejón-Ferre, Á. J., Pérez-Alonso, J., & Carreño-Ortega, Á. (2012). Greenhouse tomato production with electricity generation by roof-mounted flexible solar panels. *Scientia Agricola, 69*(4), 233–239.
Vadiee, A., & Martin, V. (2013). Energy analysis and thermoeconomic assessment of the closed greenhouse – the largest commercial solar building. *Applied Energy, 102*, 1256–1266.
Wenger, E., & Teitel, M. (2012). Design of a concentrated photovoltaic system for application in high tunnels. *Acta Horticulturae, 952*, 401–408.
Yano, A., Furue, A., Kadowaki, M., Tanaka, T., Hiraki, E., Miyamoto, M., et al. (2009). Electrical energy generated by photovoltaic modules mounted inside the roof of a north–south oriented greenhouse. *Biosystems Engineering, 103*(2), 228–238.
Yano, A., Furue, A., Moriyama, T., Ide, O., & Tsuchiya, K. (2007). Development of a greenhouse shading screen controller driven by photovoltaic energy. *Journal of the Japanese Society of Agricultural Machinery, 69*(6), 57–64 (in Japanese with English abstract).
Yano, A., Kadowaki, M., Furue, A., Tamaki, N., Tanaka, T., Hiraki, E., et al. (2010). Shading and electrical features of a photovoltaic array mounted inside the roof of an east–west oriented greenhouse. *Biosystems Engineering, 106*(4), 367–377.
Yano, A., Tsuchiya, K., Nishi, K., Moriyama, T., & Ide, O. (2007). Development of a greenhouse side-ventilation controller driven by photovoltaic energy. *Biosystems Engineering, 96*(4), 633–641.
Yano, A., Tsuchiya, K., Nishi, K., Moriyama, T., Ide, O., Ishizaka, A., et al. (2005b). Development of a power saving greenhouse side window controller driven by photovoltaic energy. *Journal of the Japanese Society of Agricultural Machinery, 67*(2), 100–110 (in Japanese with English abstract).
Yano, A., Tsuchiya, K., Nishi, K., Moriyama, T., Ide, O., & Toya, M. (2005a). Development of a photovoltaic module as a power source for greenhouse environment control devices and a study on its mounting in a greenhouse. *Journal of the Japanese Society of Agricultural Machinery, 67*(5), 124–127 (in Japanese).